RSC Advances

PAPER

View Article Online
View Journal | View Issue

Check for updates

Cite this: *RSC Adv.*, 2024, **14**, 36370

Synthesis of MOF-supported Pt catalyst with high electrochemical oxidation activity for methanol oxidation†

Merve Akin,[ab] Hatice Kars,[a] Muhammed Bekmezci,[ab] Aysenur Aygun,[a] Mert Gul,[a] Guray Kaya[b] and Fatih Sen *[a]

Received 4th September 2024
Accepted 6th November 2024

DOI: 10.1039/d4ra06393g

rsc.li/rsc-advances

Fuel cells, one of the clean energy sources, is quite remarkable for energy production. In this context, catalysts are needed for the electrochemical reactions of DMFCs (direct methanol fuel cells) to work efficiently. In this study, Pt and Pt@Ti-MOF (Pt@MIL-125) NPs (nanoparticles) catalysts were synthesized by chemical synthesis. The Ti-MOF (MIL-125) structure was synthesized using the solvothermal method, and the effect of Ti-MOF on methanol oxidation was investigated. The results showed that Pt@Ti-MOF NPs provided 9.45 times more electrocatalytic activity for methanol oxidation compared to Pt NPs. In addition, Ti-MOF doping was shown to increase the stability and durability by long-term tests. The study provides important results on how MOF-supported structures behave electrochemically. The results show that Ti-MOF provides very high potential in MOR applications and is promising for use as an anode catalyst in DMFC systems.

Open Access Article. Published on 13 November 2024. Downloaded on 2/5/2026 2:32:00 PM.
This article is licensed under a Creative Commons Attribution-NonCommercial 3.0 Unported Licence.

1. Introduction

With the increase in population, fossil fuels are one of the most used resources to meet the increasing energy demand.[1] The damage caused by fossil fuels in energy production and the decrease in resources are known to cause many problems.[2] As fossil fuels are declining and harmful to the environment, efforts are being made to provide environmentally friendly, efficient, and renewable alternative sources to generate energy.[3] Among these sources, fuel cells have recently attracted considerable attention. Fuel cells are electrochemical devices that convert the chemical energy of fuels directly into electrical energy with high efficiency.[4] Compared to rechargeable batteries, fuel cells operate continuously for longer periods and can be recharged.[5] Various fuels such as hydrogen, methane, CO, and methanol can be used in fuel cells.[6] Alcohol-based fuels are sustainable and environmentally friendly within the carbon cycle because they are derived from plant sources. In alcohol fuel cells, methanol is usually used as fuel. Methanol is liquid and easy to process and store.[7] It is also a preferred fuel because it is produced from renewable biomass resources or natural gas. The direct methanol fuel cell (DMFC) provides advantages such as high energy density, easy charging, low cost, ease of use, low toxicity, low operating temperature, and portability.[8,9] With these advantages, DMFC has become an important power source for portable electronic devices, stationary applications, and electronic vehicles.[10]

In alcohol fuel cells, energy is released as a result of redox reactions. Alcohol oxidation is an electrochemical reaction that occurs at the anode of the cell.[11] These reactions occur in the presence of some catalysts. Platinum (Pt), which has a high reaction yield, is often the preferred anode catalyst in DMFCs for methanol oxidation reaction (MOR).[12,13] However, problems such as excessive use of expensive platinum (Pt) catalysts, slow kinetics of methanol electro-oxidation reaction (MOR) at the anode, and poor stability of support materials reduce its applicability in fuel cells.[14] In addition, the CO poisoning and high cost of platinum in oxidation processes limit its use.[15,16] These limitations have led to the investigation of different catalysts.[17–19] In this context many studies such as PtRu,[20] PtCo,[21] PtNi,[22] *etc.* have been carried out. In addition, studies have been performed on the development of advanced catalysts for methanol fuel cells using trimetallic and carbon-based supports.[23] Apart from these materials, metal–organic frameworks (MOF) are porous materials and are a new generation of materials consisting of metal ions and organic binders, which have applications in many fields such as adsorption, catalysis, drug delivery, *etc.*[24–26] It can be used as a catalyst and catalyst support, especially with its high surface area and porous structure.[27] MOF-based catalyst applications can play an important role in catalyzing reactions such as fuel redox processes.[28] When MOF-based catalyst applications are examined; Zr-MOF@PANI/Ni-NPs were synthesized in a study by

[a]*Sen Research Group, Department of Biochemistry, Dumlupinar University, Kutahya, Turkey. E-mail: fatihsen1980@gmail.com*

[b]*Department of Materials Science & Engineering, Faculty of Engineering, Dumlupinar University, Kutahya, Turkey*

† Electronic supplementary information (ESI) available. See DOI: https://doi.org/10.1039/d4ra06393g

© 2024 The Author(s). Published by the Royal Society of Chemistry

Open Access Article. Published on 13 November 2024. Downloaded on 2/5/2026 2:32:00 PM.
This article is licensed under a Creative Commons Attribution-NonCommercial 3.0 Unported Licence.

Sheikhi *et al.* The obtained NP was used in methanol oxidation studies and it was attributed that the NP presented high electrocatalytic activity and there was a very good synergy between Zr-MOF, PANI, and Ni NPs. It was also reported that the surface area of the structure is high and offers a good alternative for DMFC applications.[29] In a study by Noor *et al.*, Cu-BTC MOF was hydrothermally synthesized and reported to exhibit an outstanding performance for methanol oxidation. It has been reported that it offers a very high diffusion coefficient, but its stability needs to be improved.[30] In a study by Mehek *et al.* Co-MOF-71 composites were synthesized by hydrothermal method and used for methanol oxidation studies. The results obtained were that a current density of 29.1 mA cm^{-2} at 50 mV s^{-1} was obtained, exhibited a stable structure, and may attract attention for fuel cell applications as a cost-effective catalyst.[31] Ti-MOF (MIL-125) are materials of the formula $[Ti_8O_8(OH)_4(COO)_{12}]$ with a very tunable band gap and large surface area.[32] These MOFs, which have very high chemical stability, can also show very high stability against alcohol oxidation.[33] Ti-MOF, which is especially preferred in photocatalyst applications, was used in methanol oxidation studies for the first time in this study. The selection of Ti-based MOF in the study scope was effective because titanium is stable in its oxidation state, making titanium-based MOFs more resistant to oxidation and less prone to degradation in catalytic processes. This is important for the continuation of catalytic activity in methanol oxidation. In addition, titanium contributes to structural stability and durability even under harsh conditions by forming strong bonds with organic binders in MOFs. This is important for a long-lasting fuel cell. In addition, titanium is environmentally friendly and non-toxic and has high Lewis acidity, which helps activate methanol molecules and promote their oxidation. The strong interaction between titanium and methanol positively affects catalytic performance. While Co, Cu, and Fe-based MOFs can also exhibit good catalytic performance, titanium's superior properties such as stability, non-toxicity, and photocatalytic potential offer considerable advantages for methanol oxidation.

In this study; Pt and Pt@Ti-MOF NPs were synthesized and the obtained catalysts were used for methanol oxidation studies. The obtained NPs were also characterized by XRD, TEM and EDX-Mapping. CV (cyclic voltammetry), SR (scan rate), LSV (linear sweep voltammetry), CA (chronoamperometry), 500 cycle, and EIS (electrochemical impedance spectroscopy) tests were also performed to investigate the electrocatalytic activity of the obtained NPs for methanol oxidation. It was observed how the addition of Ti-MOF to the structure affects the electrocatalytic activity in the methanol oxidation study. The results show that Pt@Ti-MOF NPs catalyst offers high potential for fuel cell anode catalyst application.

2. Material and method

2.1. Chemicals

Methanol (98%), dimethylformamide (DMF (99%)), terephthalic acid (98%), platinum(II) chloride ($PtCl_2$), isopropyl titanate, sodium borohydride ($NaBH_4$), dimethyl sulfoxide (DMSO (98%)), and Nafion were obtained from Sigma Aldrich. The chemicals purchased were of high purity and were used as received.

2.2. Synthesis of Ti-MOF (MIL-125)

MIL-125(Ti-MOF) was synthesized by the solvothermal method.[34] Briefly; 6 mL of methanol and 54 mL of DMF were mixed in a beaker. 3.53 g terephthalic acid was added to the methanol and DMF solution and stirred for 20 minutes. After terephthalic acid was dissolved, 2.1 mL of isopropyl titanate was added and stirred for 30 minutes. It was then transferred to a 100 mL polytetrafluoroethylene liner and placed in the steel autoclave apparatus. The autoclave was heated at 150 °C for 16 hours. After 16 hours, the reaction system was cooled to room temperature and centrifuged. Then, the obtained MIL-125 was dispersed in methanol and stirred for 8 hours. The final samples were dried in a vacuum oven at 60 °C for 12 hours.

2.3. Synthesis of Pt and Pt@Ti-MOF NPs

For the synthesis of Pt@Ti-MOF NPs, 80 mg of the previously prepared MIL-125 was weighed and added to 2 mL of the metal solution containing 20 mg $PtCl_2$ and mixed until a homogeneous solution was obtained. Then 20 mg (2 mL) $NaBH_4$ solution was added and stirred for 1 hour. After 1 hour, it was centrifuged at 12 000 rpm and washed with pure water. The synthesis of Pt NPs was carried out without MIL-125 by performing the above processes. The obtained Pt and Pt@MIL-125 NPs were dried at 80 °C for 12 hours.[35]

2.4. Electrochemical characterization

It is described in detail in the ESI Section.†

2.5. Material structure

It is described in detail in the ESI section.†

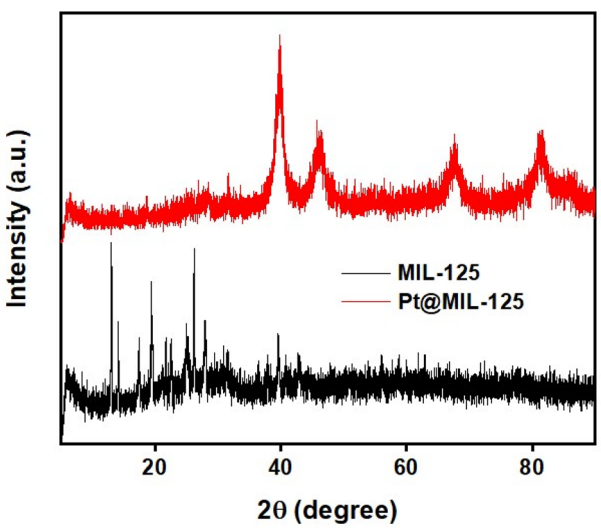

Fig. 1 XRD graph of MIL-125 and Pt@MIL-125.

Open Access Article. Published on 13 November 2024. Downloaded on 2/5/2026 2:32:00 PM.
This article is licensed under a Creative Commons Attribution-NonCommercial 3.0 Unported Licence.

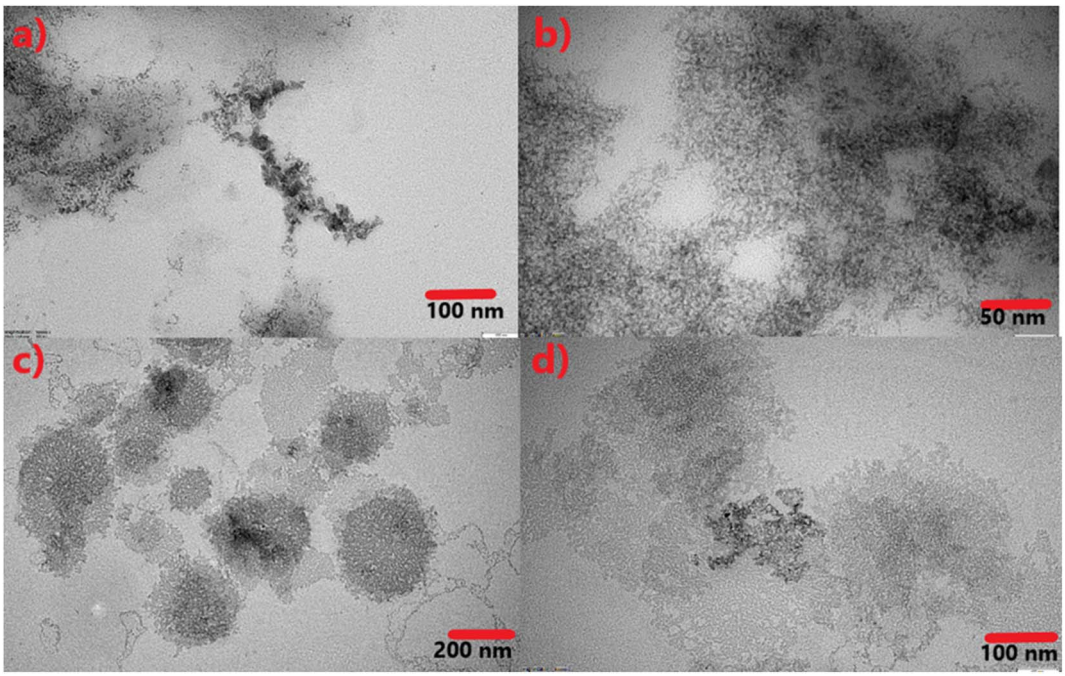

Fig. 2 Different scale TEM images of Pt (a and b) and Pt@MIL-125 (c and d).

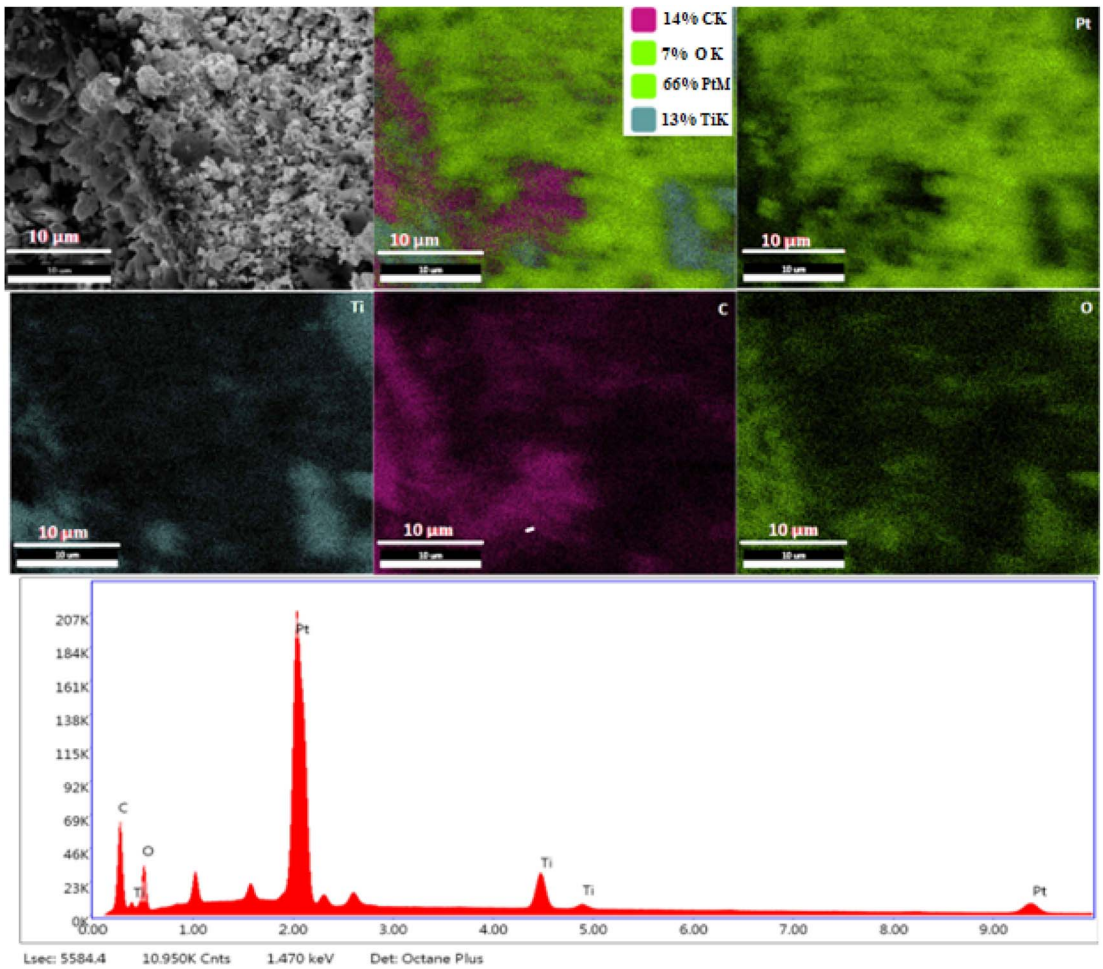

Fig. 3 EDX-mapping of Pt@MIL-125.

© 2024 The Author(s). Published by the Royal Society of Chemistry

Open Access Article. Published on 13 November 2024. Downloaded on 2/5/2026 2:32:00 PM.
This article is licensed under a Creative Commons Attribution-NonCommercial 3.0 Unported Licence.

3. Result and discussion

Fig. 1 shows the XRD analysis of MIL-125 and Pt@MIL-125 NPs. The diffraction peaks for pure MIL-125 (Ti-MOF) agree with previously reported literature.[36–39] The existence of an orthorhombic crystal structure can be mentioned for MIL-125.[40] In the literature, the angles corresponding to the (111), (200), (220), and (311) planes of Pt are reported at 39.46°, 45.24°, 67.63°, and 81.30°, respectively.[41] The diffraction peaks in the synthesized Pt@MIL-125 NPs are similar to the diffraction peaks of pure Pt NPs. The angles at 39.85°, 46.54°, 67.76°, and 81.63° corresponding to the (111), (200), (220), and (311) planes of Pt was observed for Pt@MIL-125. Besides, there was a decrease in the distinctness of the peaks belonging to MIL-125. This may be due to the low composition and high dispersion of MIL-125 (Ti-MOF) in Pt@MIL-125.[42,43]

The obtained NPs were also characterized by TEM to visualize their morphological structures. TEM images of Pt NPs are shown in Fig. 2a and b. As observed in the figure, Pt synthesized by the chemical reduction method is slightly clustered. Generally, Pt NP exhibits a morphologically smooth surface appearance. Pt@Ti-MOF nanostructures are shown in Fig. 2c and d. It shows the agglomeration of small nanoparticles after modification with MOF.[44] MOF acts as a metal–organic framework for Pt and this Pt is bound by weak bonds. TEM images also show that the MOF structure acts as a skeleton for Pt NPs and the nanoparticles appear to be dispersed on the surface. The dense Pt distributions indicate that Pt was successfully integrated into MIL-125, which could enable it to provide high performance for methanol oxidation. The results are consistent with the literature.[44]

Typical field emission scanning electron microscope (FE-SEM), EDX mapping images of Pt@MIL125 nanocomposite are shown in Fig. 3. For Pt@MIL-125(Ti-MOF), Pt NPs were found to be randomly distributed on the MIL125 surface. In the SEM images, it was observed that the MIL-125 surface became rough with the addition of Pt NPs. In the EDX-mapping results of Pt@MIL125, the coexistence of C, O, Ti and Pt was also confirmed. EDX-mapping results revealed that Pt was more dense in the Pt@MIL125 structure. EDX-mapping showed the presence of elements offering high catalytic activity potential. The results are consistent with the literature.[45]

4. Electrochemical studies

Generally, The reactions occurring in the methanol oxidation process are as follows (a)–(c).[9]

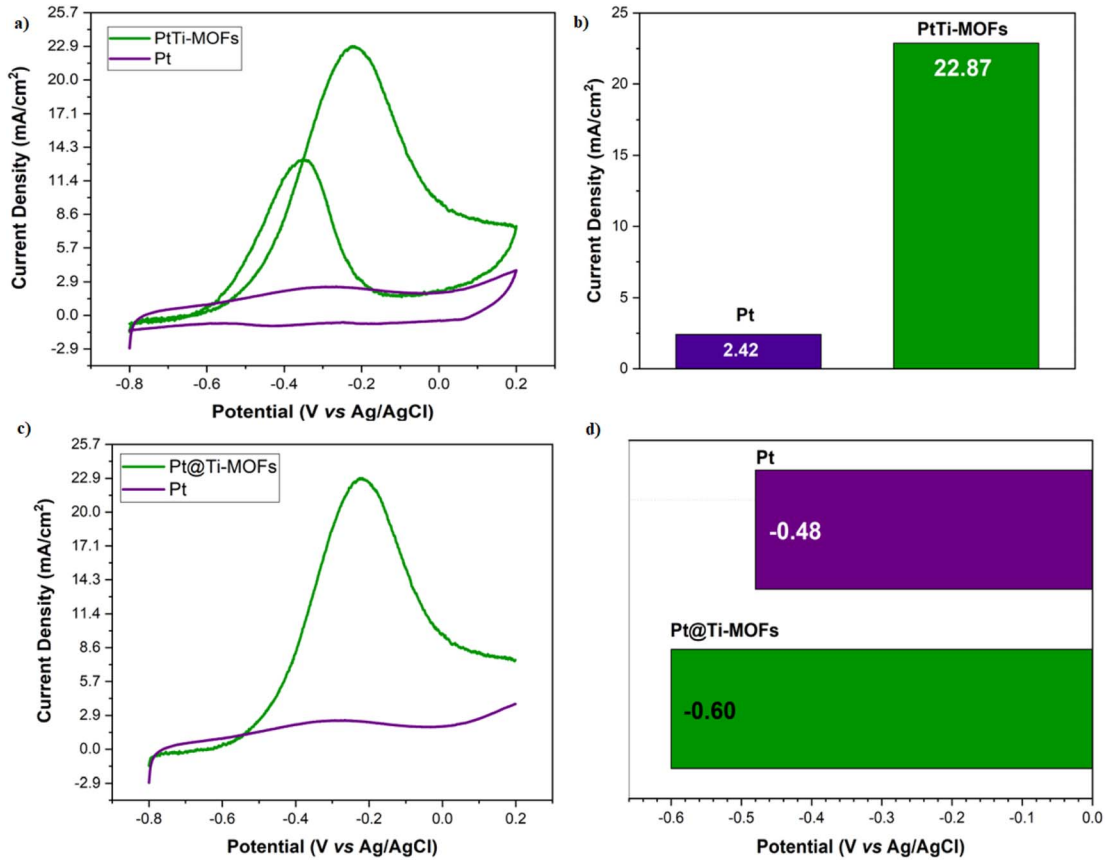

Fig. 4 (a) CV results for Pt and Pt@Ti-MOF NPs in the presence of 0.5 M KOH and 1 M CH_3OH at a scan rate of 50 mV s^{-1}, (b) methanol oxidation peak current density values for Pt and Pt@Ti-MOF NPs, (c) LSV results for Pt and Pt@Ti-MOF NPs in the presence of 0.5 M KOH and 1 M CH_3OH at 50 mV s^{-1} scan rate, (d) methanol oxidation onset potential values for Pt and Pt@Ti-MOF NPs.

Open Access Article. Published on 13 November 2024. Downloaded on 2/5/2026 2:32:00 PM.
This article is licensed under a Creative Commons Attribution-NonCommercial 3.0 Unported Licence.

$$CH_3OH + H_2O \rightarrow 6H^+ + 6e^- + CO_2 \quad \text{Anode reaction (a)}$$

$$3/2O_2 + 6H + 6e^- \rightarrow 2H_2O \quad \text{Cathode reaction (b)}$$

$$CH_3OH + 3/2O_2 \rightarrow CO_2 + 2H_2O \quad \text{General reaction (c)}$$

Cyclic Voltammettry (CV), Scan Rate (SR), long-term (500 cycles), Chronoamperometry (CA) and Electrochemical Impedance Spectrometry (EIS) measurements were performed for the electrochemical studies of Pt and Pt@Ti-MOF NPs obtained within the scope of the study. CV measurements were performed in 0.5 M KOH buffer solution in the range of −0.8 V–0.2 V. In the presence of 1 M CH_3OH; the results of the CV graphs obtained are as shown in Fig. 4a. In the obtained results; oxidation current densities of 2.42 mA cm^{-2} and 22.87 mA cm^{-2} were obtained for Pt and Pt@Ti-MOF NPs, respectively (Fig. 4b). This showed that Pt@Ti-MOF catalyst provided 9.45 times more electrocatalytic activity than Pt NPs. In addition, the Linear Sweep Voltammetery (LSV) results of the obtained catalysts are shown in Fig. 4c. According to these results, the oxidation peaks of Pt and Pt@Ti-MOF NPs catalysts started at −0.48 V and −0.6 V, respectively. This showed that Ti-MOFs were effective in starting the oxidation process earlier in the catalyst. It also shows that the oxidation process takes place more easily on the surface of the Pt@Ti-MOF NPs catalyst.

Fig. 5 shows the current densities and R^2 values obtained at different scan rates for Pt and Pt@Ti-MOF NPs catalysts. The measurements were performed in the potential range of −0.8 V–0.2 V and at scan rates of 50 mV s^{-1}, 100 mV s^{-1}, 150 mV s^{-1}, 200 mV s^{-1}, 250 mV s^{-1} and 300 mV s^{-1}. The results showed that for both catalysts, the current densities increased with increasing scan rate. This indicated the existence of diffusion-controlled systems. At the same time, it gave information that methanol oxidation can be controlled by mass transport in the obtained systems. In addition, the obtained results supported the CV results by observing that the Pt@Ti-MOF NPs catalyst provided higher electrocatalytic activity as the scan rate increased.

In Fig. 6a, CA test was performed to investigate the stability of Pt and Pt@Ti-MOF NPs catalysts. The measurements were carried out for 5000 s in the presence of 0.5 M KOH and 1 M CH_3OH. The results showed a rapid decrease in the current density of Pt NPs. This can be attributed to the occurrence of poisoning of the catalyst in methanol oxidation. For the Pt@Ti-MOF NPs catalyst, the current density was slower, and at the end of 5000 s, a current density of about 3 mA cm^{-2} was observed. This indicated that the addition of Ti-MOF to the catalyst increased the stability considerably and the methanol oxidation continued. Fig. 6b shows the EIS results of the catalysts. In EIS measurements; the semicircle diameter in Nyquist plots is

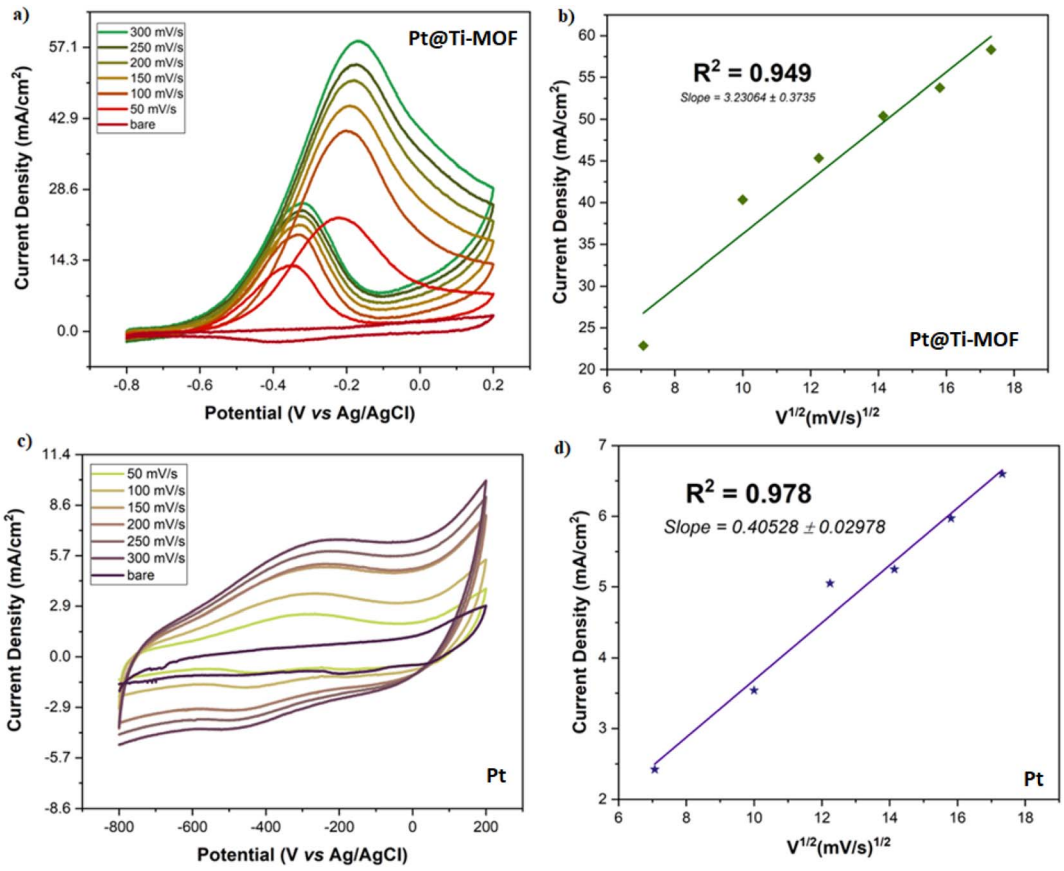

Fig. 5 (a) Scan rate measurements for Pt@Ti-MOF NPs obtained at scan rates of 50 mV s^{-1}, 100 mV s^{-1}, 150 mV s^{-1}, 200 mV s^{-1} and 250 mV s^{-1}, (b) correlation graph obtained with scan rate results for Pt@Ti-MOF NPs, (c) scan rate measurements for Pt NPs obtained at scan rates of 50 mV s^{-1}, 100 mV s^{-1}, 150 mV s^{-1}, 200 mV s^{-1} and 250 mV s^{-1}, (d) correlation graph obtained with scan rate results for Pt NPs.

© 2024 The Author(s). Published by the Royal Society of Chemistry

Open Access Article. Published on 13 November 2024. Downloaded on 2/5/2026 2:32:00 PM.
This article is licensed under a Creative Commons Attribution-NonCommercial 3.0 Unported Licence.

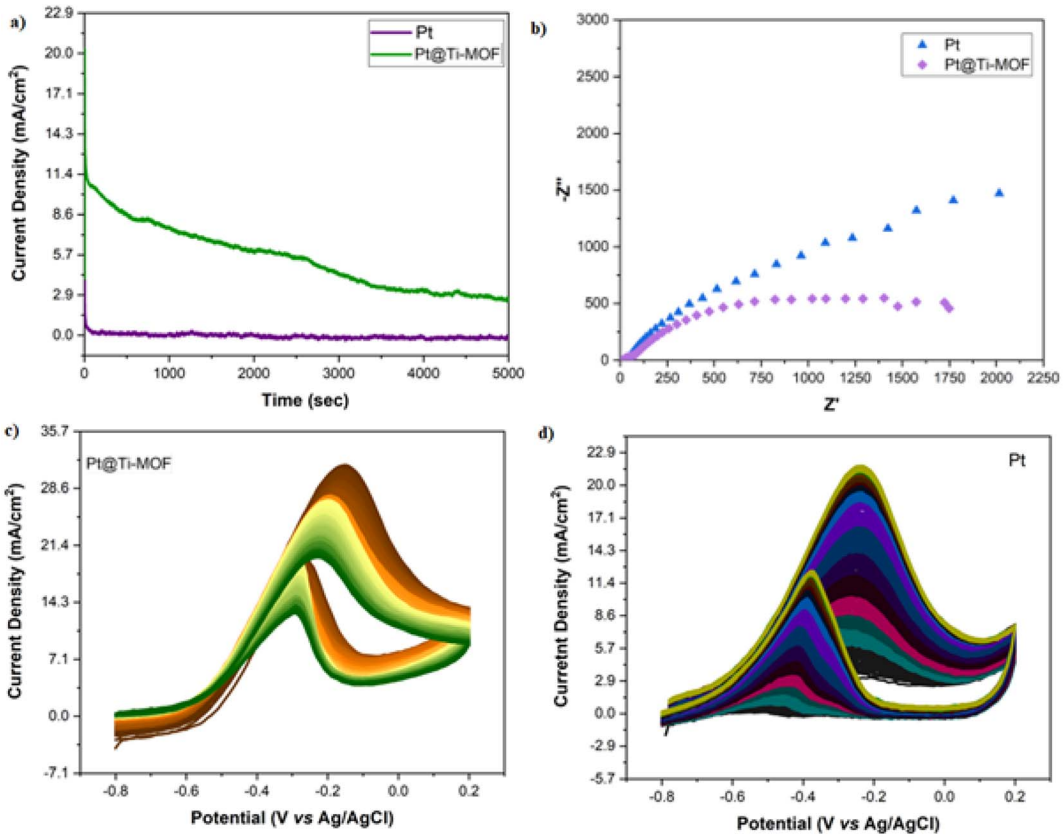

Fig. 6 (a) CA measurement results of the obtained catalysts in 0.5 M KOH buffer solution containing 1 M CH_3OH at 50 mV s^{-1}, (b) Nyquist plots for Pt and Pt@Ti-MOF NPs in 0.5 M KOH buffer solution containing 1 M CH_3OH, (c) 500 cycles measurement for Pt@Ti-MOF NPs, (d) 500 cycles measurement for Pt NPs.

associated with the charge transfer resistance. Accordingly, the smaller circle diameter of the Pt@Ti-MOF catalyst showed that the methanol oxidation reaction was faster. This also supported the LSV results. Fig. 6c and d shows the long-term stability test results. Measurements were performed in the presence of 1 M CH_3OH and 0.5 M KOH at a scan rate of 50 mV s^{-1}. The results showed that the Pt@Ti-MOF NPs catalyst increased up to a current density of approximately 33 mA cm^{-2} but after a certain period, the current density decreased. In the Pt NPs catalyst, an increase in current density was observed during 500 cycles. In addition, when the I_f (forward scan), and I_b (reverse scan) current peaks were examined during 500 cycles; it was observed that an increase in I_b current occurred during 500 cycles in the Pt catalyst. This suggests that the CO poisoning tolerance is low and the presence of intermediate product formation. It was also observed that the I_f/I_b ratio calculated at cycle 500 for Pt and Pt@Ti-MOF catalysts decreased by 1.98 and 1.19 times compared to the I_f/I_b ratio calculated at cycle 1, respectively. This indicates that the addition of Ti-MOF to the catalyst increases the poisoning tolerance and gives more stable results. The results are also consistent with CA results.

Table 1 Comparison of current densities obtained from different catalysts

Electrocatalyst	Medium	Alcohol	Scan rate mV s^{-1}	Peak current (mA cm^{-2})	Reference
Pt_1Fe_1@NC/MWCNTs	0.1 M $HClO_4$	0.5 M CH_3OH	50	18.19	46
Pt–Pd	0.5 M H_2SO_4	1 M CH_3OH	50	0.67	47
$PtFe_3O_4$@GA	1 M KOH	1 M CH_3OH	50	37.25	48
NiFe-LDH/Pt	0.5 M KOH	1 M CH_3OH	50	18	49
ZrO_2/NiO/rGO	0.5 M KOH	0.7 M CH_3OH	20	26.6	50
Pt/C	1 M KOH	1 M CH_3OH	50	10.5	51
5 wt% GO/Co-MOF-71	1 M KOH	3 M CH_3OH	50	29.1	31
PtCuCo NPs	0.5 M H_2SO_4	1 M CH_3OH	50	4.24	52
Pt@LLG	1 M H_2SO_4	1 M CH_3OH	50	57.73	53
Pt GA^{-1}	0.5 M H_2SO_4	0.5 M CH_3OH	50	8.72	54
Pt@Ti-MOF	0.5 M KOH	1 M CH_3OH	50	21	This work

© 2024 The Author(s). Published by the Royal Society of Chemistry

Open Access Article. Published on 13 November 2024. Downloaded on 2/5/2026 2:32:00 PM.
This article is licensed under a Creative Commons Attribution-NonCommercial 3.0 Unported Licence.

Within the scope of this study; Pt@Ti-MOF NPs catalyst was synthesized to eliminate some of the disadvantages of Pt in fuel cells and to reduce its cost. In addition, the effect of Ti-MOF on methanol oxidation was investigated by comparing it with the obtained Pt catalyst. The results obtained indicate that Pt@Ti-MOF NPs form a good synergy and provide high catalytic activity. In addition, the methanol oxidation peaks obtained in other studies in the literature are compared in Table 1. The comparisons showed that the Ti-MOF support provided higher electrocatalytic activity than supports such as Pd and Graphene Aerogel (GA) and some trimetallic structures. It is also predicted that the obtained catalyst will provide higher catalytic activity by supporting different structures. When compared with commercial Pt/C NPs, it is seen that the obtained catalyst provides 2 times more electrocatalytic activity. The results are in agreement with the literature and show that Ti-MOF NPs show high potential in fuel cell anode catalysis and exhibit properties that can be used for the development of catalysts.

5. Conclusion

In this study, Pt and Pt@Ti-MOF catalysts were synthesized by chemical reduction method and Ti-MOF structure by solvothermal method. The synthesized catalysts were characterized by XRD, TEM and EDX-Mapping. CV, SR, LSV, CA, 500 cycle, and EIS tests were performed to investigate the electrocatalytic activity of the obtained NPs in methanol oxidation. The results obtained, it was aimed to investigate the effect of Ti-MOF on methanol oxidation. According to the results obtained; the Pt@Ti-MOF catalyst showed 9.45 times higher catalytic activity than the Pt catalyst. It was also observed that it showed longer stability compared to the CA test and methanol oxidation continued at the end of 5000 s. According to EIS results; it was observed that methanol oxidation mass transfer was faster stability was increased and CO tolerance was higher with 500 cycle tests. The results showed that Ti-MOF exhibited electrocatalytic performance 2 times higher than commercial Pt/C and offered high potential for use as a fuel cell anode catalyst.

Data availability

Data from this study will be made available upon request.

Conflicts of interest

There are no conflicts to declare.

Acknowledgements

Muhammed Bekmezci would like to thank the TUBITAK 2211-C PhD Priority Areas Scholarship Program. No. Funded. The authors also would like to thank to DPU BAP (2018-29) for chemicals.

References

1 A. N. Celik, *Düzce Üniversitesi Bilim ve Teknol. Derg.*, 2021, **9**, 500–519.
2 J. Wang and W. Azam, *Geosci. Front.*, 2024, **15**, 101757.
3 K. K. Jaiswal, C. R. Chowdhury, D. Yadav, R. Verma, S. Dutta, K. S. Jaiswal, B. Sangmesh and K. S. K. Karuppasamy, *Energy Nexus*, 2022, **7**, 100118.
4 A. G. Olabi, T. Wilberforce and M. A. Abdelkareem, *Energy*, 2021, **214**, 118955.
5 N. Sazali, W. N. W. Salleh, A. S. Jamaludin and M. N. M. Razali, *Membranes*, 2020, **10**, 99.
6 A. Kaur, G. Kaur, P. P. Singh and S. Kaushal, *Int. J. Hydrogen Energy*, 2021, **46**, 15820–15849.
7 M. S. Alias, S. K. Kamarudin, A. M. Zainoodin and M. S. Masdar, *Int. J. Hydrogen Energy*, 2020, **45**, 19620–19641.
8 Z. K. Coguplugil, M. Akin, R. Bayat, M. Bekmezci, H. Karimi-Maleh, A. Javadi and F. Sen, *Int. J. Hydrogen Energy*, 2023, **48**, 21285–21293.
9 L. Yaqoob, T. Noor and N. Iqbal, *Int. J. Energy Res.*, 2021, **45**, 6550–6583.
10 M. B. Askari, P. Salarizadeh, M. Seifi and S. M. Rozati, *Solid State Sci.*, 2019, **97**, 106012.
11 M. Bekmezci, E. E. Altuner, V. Erduran, R. Bayat, I. Isik and F. Şen, in *Nanomaterials for Direct Alcohol Fuel Cells*, Elsevier, 2021, pp. 1–15.
12 W. Lou, A. Ali and P. K. Shen, *Nano Res.*, 2022, **15**, 18–37.
13 Z. Li, X. Jiang, X. Wang, J. Hu, Y. Liu, G. Fu and Y. Tang, *Appl. Catal., B*, 2020, **277**, 119135.
14 V. T. T. Phan, T. M. Pham, H. Q. Pham, T. T. Huynh, T. H. T. Nguyen and V. T. T. Ho, *Int. J. Energy Res.*, 2022, **46**, 19221–19232.
15 F. Karimi, M. Akin, R. Bayat, M. Bekmezci, R. Darabi, E. Aghapour and F. Sen, *Mol. Catal.*, 2023, **536**, 112874.
16 H. Tian, Y. Yu, Q. Wang, J. Li, P. Rao, R. Li, Y. Du, C. Jia, J. Luo, P. Deng, Y. Shen and X. Tian, *Int. J. Hydrogen Energy*, 2021, **46**, 31202–31215.
17 A. Q. K. Nguyen, H. Q. Pham, S. T. M. Huynh and T. T. Huynh, *Adv. Sustainable Syst.*, 2023, **2300205**, 1–30.
18 T. T. Huynh, H. Q. Pham, A. Van Nguyen, L. G. Bach and V. T. T. Ho, *Ind. Eng. Chem. Res.*, 2019, **58**, 675–684.
19 V. T. T. Ho, H. Q. Pham, T. H. T. Anh, A. Van Nguyen, K. A. N. Quoc, H. T. H. Vo and T. T. Nguyen, *C. R. Chim.*, 2019, **22**, 838–843.
20 W. Qiao, X. Huang and L. Feng, *Chin. J. Struct. Chem.*, 2022, **41**, 2207016–2207034.
21 H. Burhan, H. Ay, E. Kuyuldar and F. Sen, *Sci. Rep.*, 2020, **10**, 1–8.
22 X. Chen, J. Zhao, J. Lian and X. Wang, *Green Chem.*, 2023, **25**, 3198–3207.
23 H. Huang and X. Wang, *J. Mater. Chem. A*, 2014, **2**, 6266–6291.
24 V. R. Bakuru, M. E. DMello and S. B. Kalidindi, *ChemPhysChem*, 2019, **20**, 1177–1215.
25 N. A. Khan, Z. Hasan and S. H. Jhung, *Coord. Chem. Rev.*, 2018, **376**, 20–45.

© 2024 The Author(s). Published by the Royal Society of Chemistry

Open Access Article. Published on 13 November 2024. Downloaded on 2/5/2026 2:32:00 PM.
This article is licensed under a Creative Commons Attribution-NonCommercial 3.0 Unported Licence.

26 S. Sanati, R. Abazari, A. Morsali, A. M. Kirillov, P. C. Junk and J. Wang, *Inorg. Chem.*, 2019, **58**, 16100–16111.
27 L. Yaqoob, T. Noor, N. Iqbal, H. Nasir and A. Mumtaz, *Sci. Rep.*, 2021, **11**, 1–18.
28 Z. Zhou, J. Zhang, S. Mukherjee, S. Hou, R. Khare, M. Döblinger, O. Tomanec, M. Otyepka, M. Koch, P. Gao, L. Zhou, W. Li and R. A. Fischer, *Chem. Eng. J.*, 2022, **449**, 137888.
29 S. Sheikhi and F. Jalali, *Fuel*, 2021, **296**, 120677.
30 T. Noor, M. Ammad, N. Zaman, N. Iqbal, L. Yaqoob and H. Nasir, *Catal. Lett.*, 2019, **149**, 3312–3327.
31 R. Mehek, N. Iqbal, T. Noor, H. Nasir, Y. Mehmood and S. Ahmed, *Electrochim. Acta*, 2017, **255**, 195–204.
32 P. Qiu, Y. Yao, S. Lu, L. Chen, Y. Chen and X. Liao, *Fuel*, 2023, **351**, 129043.
33 S. Yuan, L. Feng, K. Wang, J. Pang, M. Bosch, C. Lollar, Y. Sun, J. Qin, X. Yang, P. Zhang, Q. Wang, L. Zou, Y. Zhang, L. Zhang, Y. Fang, J. Li, H.-C. Zhou, S. Yuan, L. Feng, K. Wang, J. Pang, M. Bosch, C. Lollar, Y. Sun, J. Qin, X. Yang, P. Zhang, Q. Wang, L. Zou, Y. Zhang, L. Zhang, Y. Fang, J. Li and H. Zhou, *Adv. Mater.*, 2018, **30**, 1704303.
34 N. Li, X. Liu, J. Zhou, W. Chen and M. Liu, *Chem. Eng. J.*, 2020, **399**, 125782.
35 M. Bekmezci, G. N. Gules, R. Bayat and F. Sen, *Anal. Methods*, 2023, **15**, 1223–1229.
36 X. Han, X. Yang, G. Liu, Z. Li and L. Shao, *Chem. Eng. Res. Des.*, 2019, **143**, 90–99.
37 B. Zhai, Y. Chen and Y. Liang, *J. Nanoparticle Res.*, 2019, **21**, 1–15.
38 P. Wang, J. Lang, D. Liu and X. Yan, *Chem. Commun.*, 2015, **51**, 11370–11373.
39 J. Li, X. Shan, D. Jiang, W. Wang and Z. Chen, *Microchim. Acta*, 2020, **187**, 1–8.
40 Y. Zhao, W. Cai, J. Chen, Y. Miao and Y. Bu, *Front. Chem.*, 2019, **7**, 490118.
41 Y. Kocak, A. Aygun, E. E. Altuner, S. Ozdemir, S. Gonca, D. Berikten, R. N. E. Tiri and F. Sen, *Int. J. Environ. Sci. Technol.*, 2023, 1–12.
42 S. Yin, Y. Chen, Q. Hu, M. Li, Y. Ding, J. Di, J. Xia and H. Li, *Res. Chem. Intermed.*, 2020, **46**, 3311–3326.
43 J. Du, J. Zhang, T. Yang, R. Liu, Z. Li, D. Wang, T. Zhou, Y. Liu, C. Liu and G. Che, *Catalysts*, 2021, **11**, 24.
44 M. Kaur, S. K. Mehta and S. K. Kansal, *Mater. Chem. Phys.*, 2020, **254**, 123539.
45 X. Liu, J. Fei, X. Peng, L. Jiang, X. Yuan, J. Yang and H. Wang, *Water, Air, Soil Pollut.*, 2023, **234**, 1–22.
46 Z. Wang, S. Zhou, W. Liao, Q. Zhou, M. Chen, J. Long and Q. Wang, *Chem.–A Eur. J.*, 2022, **28**, e202201987.
47 Y. Yang, Y. Cao, L. Yang, Z. Huang and N. V. Long, *Nanomater.*, 2018, **8**, 208.
48 M. Akin, M. Bekmezci, R. Bayat, I. Isik and F. Sen, *Fuel*, 2024, **357**, 129771.
49 L. Li, Y. Yang, Y. Wang, M. Liang and Y. Huang, *J. Mater. Res. Technol.*, 2020, **9**, 5463–5473.
50 M. B. Askari, H. Beitollahi, B. Di, A. Methanol, M. B. Askari, H. Beitollahi and A. Di Bartolomeo, *Nanomaterials*, 2023, **13**, 679.
51 H. Rostami, A. A. Rostami and A. Omrani, *Electrochim. Acta*, 2016, **191**, 536–547.
52 Y. Ren, Z. Zang, C. Lv, B. Li, L. Li, X. Yang, Z. Lu, X. Yu and X. Zhang, *J. Colloid Interface Sci.*, 2023, **640**, 801–808.
53 V. Erduran, R. Bayat, I. Isik, T. Bayazit and F. Şen, *ACS Eng. Au*, 2023, **3**, 537–545.
54 M. S. Çögenli and A. Bayrakçeken Yurtcan, *Int. J. Hydrogen Energy*, 2020, **45**, 650–666.

© 2024 The Author(s). Published by the Royal Society of Chemistry